

NASA Technical Memorandum 4733

# Analytical and Experimental Verification of a Flight Article for a Mach-8 Boundary-Layer Experiment

W. Lance Richards and Richard C. Monaghan

March 1996



NASA Technical Memorandum 4733

# Analytical and Experimental Verification of a Flight Article for a Mach-8 Boundary-Layer Experiment

W. Lance Richards and Richard C. Monaghan  
*Dryden Flight Research Center*  
*Edwards, California*



National Aeronautics and  
Space Administration  
Office of Management  
Scientific and Technical  
Information Program

1996

## **ABSTRACT**

Preparations for a boundary-layer transition experiment to be conducted on a future flight mission of the air-launched Pegasus<sup>®</sup> rocket are underway. The experiment requires a flight-test article called a glove to be attached to the wing of the Mach-8 first-stage booster. A three-dimensional, nonlinear finite-element analysis has been performed and significant small-scale laboratory testing has been accomplished to ensure the glove design integrity and quality of the experiment. Reliance on both the analysis and experiment activities has been instrumental in the success of the flight-article design. Results obtained from the structural analysis and laboratory testing show that all glove components are well within the allowable thermal stress and deformation requirements to satisfy the experiment objectives.

## **INTRODUCTION**

The prediction of boundary-layer transition for three-dimensional flow is essential to the design and development of hypersonic vehicles. Accurate transition assumptions must be made in the vehicle design because of extreme differences in the aerodynamic heating between fully-turbulent and fully-laminar flow at hypersonic speeds. If the conservative (but unrealistic) assumption of fully-turbulent flow is assumed throughout the mission, the resulting design will be extremely inefficient. Conversely, fully-laminar flow cannot be assumed for the safe design of the vehicle. Therefore, accurate assumptions concerning boundary-layer transition must be made for the vehicle design to be both efficient and robust.

Preparations for a future flight experiment are currently underway to improve crossflow-transition prediction methods for actual hypersonic flight conditions because wind-tunnel testing has not been historically feasible, e.g. Bertilrud, et al.<sup>1</sup> Crucial to the success of the experiment is the ability to design, analyze, and fabricate a fully-instrumented flight-test fixture that can provide a smooth, three-dimensional, structurally stable aerodynamic surface; and to determine when and where boundary-layer transition occurs during the flight.

To achieve these objectives, a flight-test article called a glove has been designed, analyzed, manufactured, and installed on the wing of the air-launched Pegasus<sup>®</sup> (Orbital Sciences Corporation, Fairfax, Virginia) space booster. A comprehensive structural test and analysis program has been successfully completed to validate the integrity of the complex glove design. Complexity of the design stemmed from the use of nontraditional engineering materials, geometrically complex components, transiently varying boundary conditions, and nontrivial manufacturing processes. This paper presents the glove design and describes the test and analysis details that were essential in the glove verification process.

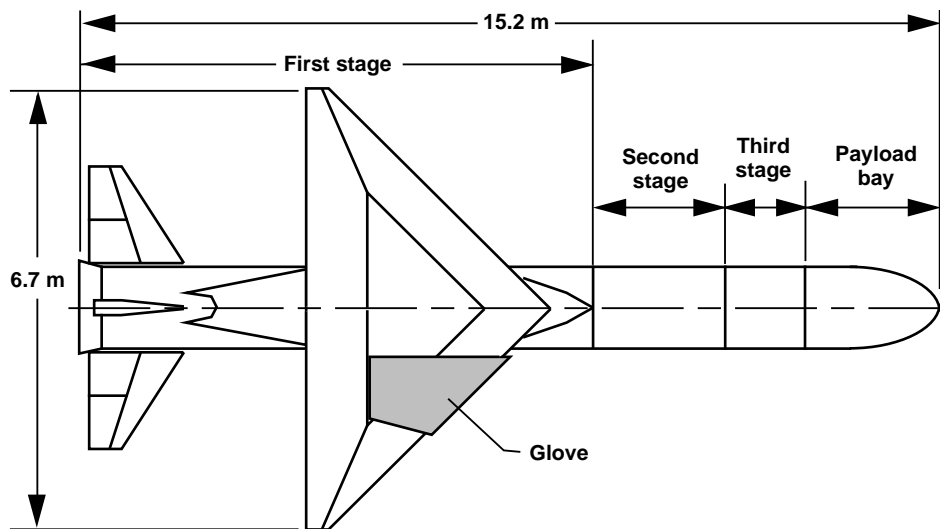
## **DESIGN REQUIREMENTS**

The glove was designed to provide valuable boundary-layer transition data during a typical Mach-8 flight of the Pegasus<sup>®</sup> space booster. This section describes the key requirements for the glove design.

### **Vehicle and Mission Requirements**

The Pegasus<sup>®</sup> is a multistaged, air-launched rocket designed to economically place small payloads into low Earth orbit. Figure 1 shows the physical dimensions of the rocket and the location of the glove. Figure 2 shows a photograph of the Pegasus<sup>®</sup> space booster mounted under the wing of a B-52 carrier aircraft.

The booster follows a fixed trajectory that is predetermined for a particular payload requirement. For a typical mission, the booster separates from the carrier aircraft at Mach 0.8 and an altitude of approximately 13,000 m and descends for 5 sec. Then, the first stage ignites. After approximately 70 sec, the vehicle has accelerated to Mach 8 and an altitude of approximately 61,000 m. After first-stage burnout occurs, the glove experiment concludes as the entire first stage is jettisoned and second-stage ignition occurs.



960002

Figure 1. Plan view of the Pegasus<sup>®</sup> XL space booster with glove.



EC89 309-3

Figure 2. Pegasus<sup>®</sup> space booster mounted under the wing of the B-52 aircraft.

### Aerothermal Loads Analysis

A vehicle trajectory, similar to those previously described, e.g. Noffz, et al.<sup>2</sup> and Noffz, et al.,<sup>3</sup> was used as input to an aero/thermal analysis to determine aerodynamic heating loads applied to the glove during the flight. An engineering aerodynamic heating code was used to calculate heat-transfer coefficients, heating rates, skin friction, and surface-static pressures at discrete locations during the transient-heating profile. The program permitted the

use of different theories for calculating heat transfer at various glove locations and flow conditions. Additional details of the aerothermal analyses performed in the glove design have previously been provided, e.g. Gong, et al.<sup>4</sup> Several combinations of glove skin thickness and materials were used in the analysis to begin defining an appropriate glove configuration.

### Structural Design Requirements

Structural design requirements included a surface waviness criterion not to exceed 0.008 cm over a 5-cm length throughout the flight envelope; a requirement to minimize any step discontinuities at the inboard edge of the test surface, especially near the leading edge; and a requirement to have a thermally conductive thin skin. Such a skin was needed so that thermocouples installed on the inside skin surface would sense heating-rate changes caused by boundary-layer transition. Weight was a secondary design consideration, and the structure was not optimized in this regard.

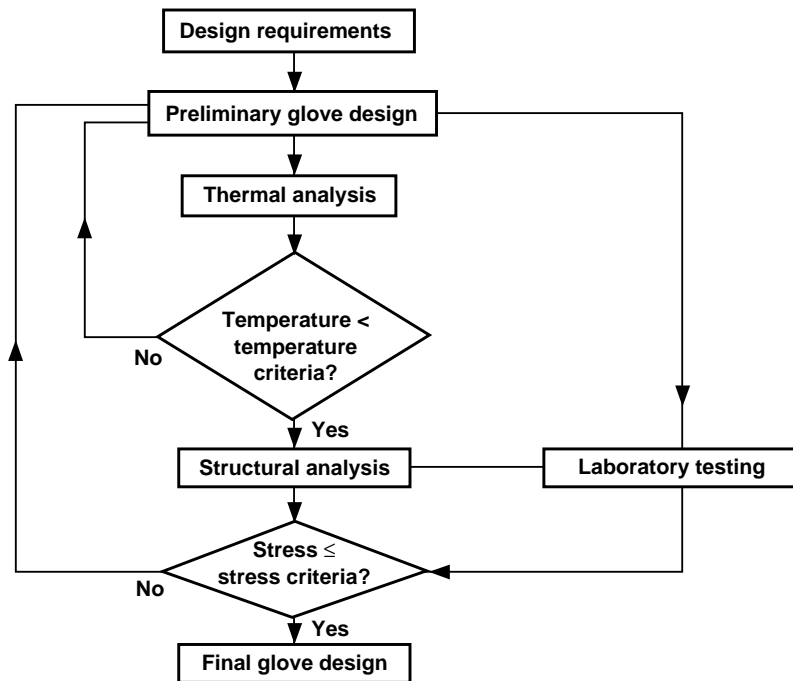
Preliminary studies showed that if the glove was rigidly constrained during heating, the test skin would buckle, or the rigid attachments would yield, or both. Thermal expansion and contraction capability was therefore regarded as an important feature in the glove design.

### Aerodynamic Design Requirements

Aerodynamic requirements such as those previously described, e.g. Godil & Bertilrud,<sup>5</sup> were also important to the design but are beyond the scope of this paper.

## PRELIMINARY DESIGN AND THERMAL ANALYSIS

Figure 3 shows the design and verification process for the design of the hypersonic glove test article. After the design requirements were defined, a preliminary design of the glove was initiated. Such a design required the



960001

Figure 3. Glove design process.

selection of materials, definition of boundary constraints, sizing of skin thicknesses and fasteners, and laying out of instrumentation and sensor wiring. The details of the initial glove design and preliminary results from the one- and two-dimensional thermal analyses that supported these tasks have previously been documented, e.g. Gong, et al.<sup>4</sup>

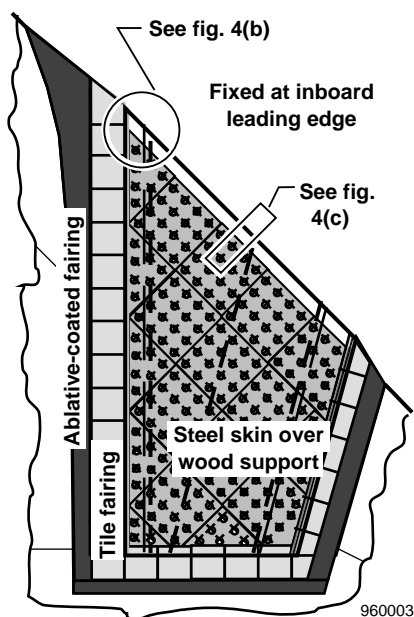
Thermal analyses of the preliminary glove design were performed to predict the glove transient-temperature response during the mission. The applied heating rates from the aerodynamic heating analysis described previously were coupled with the thermal response of the preliminary glove design. The transient-temperature distributions were then evaluated to determine if any area of the glove exceeded maximum temperature limits. Those areas in the glove design that exceeded these criteria were modified and reanalyzed until all the glove materials and structures were below maximum operating temperature criteria.

## GLOVE DESIGN

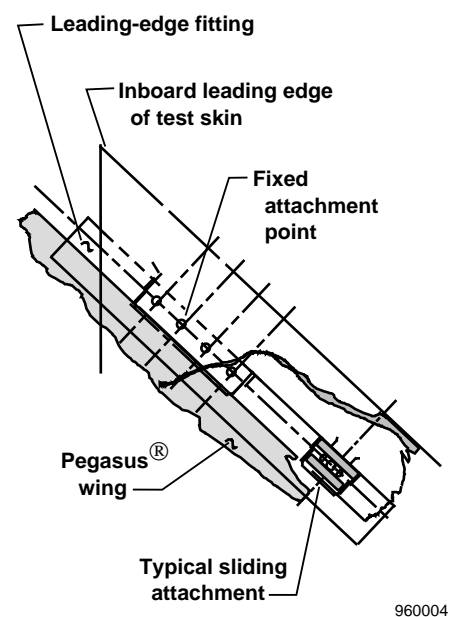
The iterative process between the preliminary design and thermal analyses resulted in a glove with a relatively thick, metallic outer skin and a large leading-edge heat sink to accommodate the extreme leading-edge heating during flight. The aerodynamic fairing that blends the metallic portion of the glove to the existing Pegasus<sup>®</sup> composite wing has previously been described, e.g. Gong, et al.<sup>4</sup>

As previously mentioned, the ability to accommodate thermal growth and contraction during flight was an important requirement for the glove. To achieve this capability, the leading edge was rigidly fixed at a single point and the metallic skin was allowed to freely expand over a balsa wood support foundation during heating.

Figure 4(a) shows a top view of the glove. Figure 4(b) shows the inboard leading edge highlighted. The single rigid attachment at the inboard leading edge and the expansion joints in the outboard direction are also shown. The preliminary design constrained the movement of the glove leading edge in the direction normal to the Pegasus<sup>®</sup> wing leading edge. However, a series of slotted attachments allowed movement in the direction parallel to the Pegasus<sup>®</sup> wing leading edge. The rigid attachment of the glove leading edge forced all thermal growth of the glove aft and parallel to the leading edge. This approach ensured glove dimensional stability at the leading edge where boundary-layer transition is the most sensitive.



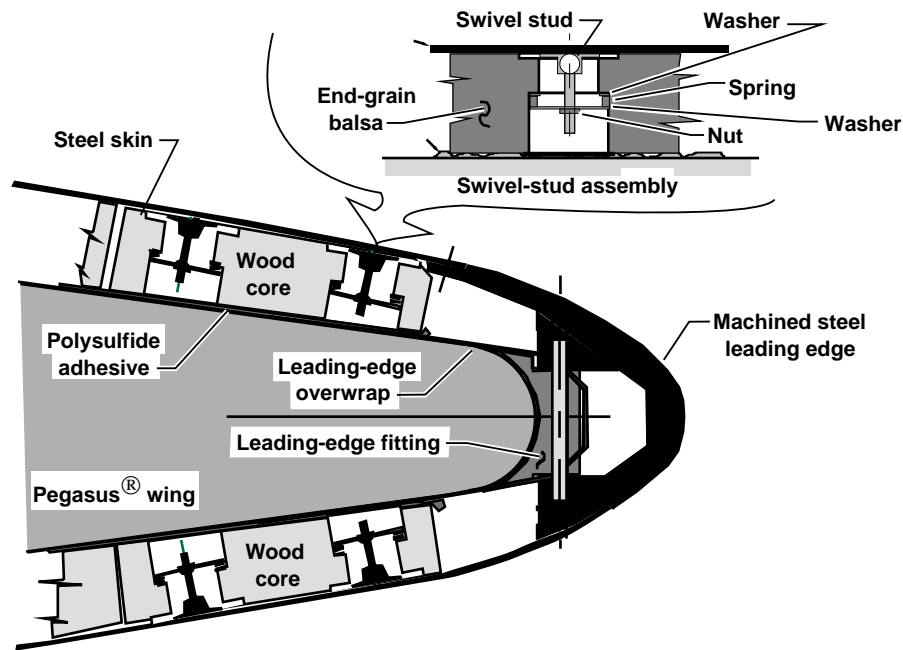
(a) Plan view of glove assembly.



(b) Glove leading-edge fixes and sliding attachment.

Figure 4. Glove assembly.

The glove outer skin consists of a nickel-plated low-carbon steel sheet that has a plan view area of approximately 1 m<sup>2</sup> (fig. 4(a)). The upper and lower skins are 0.23- and 0.35-cm thick, respectively. These skins are attached to the wing at 270 independent locations by spring-loaded swivel studs designed specifically for this flight program. Figure 4(c) shows a cross-sectional view of the glove and an enlargement of a typical swivel-stud mechanism. The swivel studs, spaced 6.4 cm apart, are bonded to the steel skins with high-temperature epoxy. To react against aerodynamic forces, the studs are preloaded to 111 N through the spring attachments to the balsa substructure. The balsa glove structure is preshaped and bonded to the outer skin of the basic Pegasus<sup>®</sup> wing. This attachment method holds the skin securely to the surface but also allows the skin to expand thermally with only a small resistance caused by sliding friction.



960005

(c) Glove internal assembly.

Figure 4. Concluded.

## SMALL-SCALE LABORATORY TESTING

The structural design of the glove incorporated unconventional construction methods and materials. Consequently, extensive small-scale laboratory testing was performed to verify those areas in the glove that possessed the greatest design uncertainty or areas that were impractical to model analytically. This section describes the two main areas on the glove that were evaluated: the joint between the upper skin and leading-edge mass (the upper joint), and the sliding attachment of the test skin to the wing. In all, more than 20 small-scale laboratory tests were performed.

### Solder-Joint Strength and Performance Tests

The requirements for the upper joint included smoothness of the aerodynamic test surface, predictable heat transfer, and fail-safety design under potentially high thermal stresses. To satisfy these requirements, the upper joint was redundantly designed with two fastening mechanisms. Solder was used to provide predictable heat transfer and a means of smoothing the joint without causing thermal conduction discontinuities. Two rows of 3-mm screws spaced at 1.3 cm in each row were also added to the joint to provide redundancy and predictable strength values for analysis of the primary structural load path.

Figure 5 shows the test article used to develop the manufacturing technique and gain confidence in the integrity of the upper-joint design. This test article consisted of a 25 cm-long section of the full-scale leading-edge mass attached by a representative joint to a 65-cm<sup>2</sup> section of the upper skin. This test article was used to develop the solder process, the joint smoothing technique, and the nickel-plating process. A pass-fail thermal stress test was also conducted on this test article.

Preliminary joint analysis had indicated that the thermal stress in the joint would be only slightly less severe on the 25-cm specimen than on the full-scale article. A representative thermal gradient was applied to this test article to demonstrate survivability of the joint. This test produced temperatures in the soldered and bolted joint similar to the predicted flight condition and produced a similar thermal gradient across the joint. The leading-edge mass was heated to 102 °C, and the thin skin was heated to 193 °C. Post-test inspection using visual and dye-penetrant techniques indicated no damage to the joint.

### **Bolt-Shear Tests in the Upper-Skin Joint**

The upper-joint design called for bolts to be shear-loaded in the threaded section, which is not standard engineering practice, and therefore, no strength data were available from existing sources. Bolt-shear tests using the actual joint materials (low-carbon steel and 793-MPa tensile-strength bolts) were conducted to determine shear strength as well as to observe the yielding characteristics. The test results indicated large margins of safety (40 percent) and significant yielding in the skin material prior to bolt failure. Bolt failure occurred from a combination of shear and bending stresses. The bolt strength was adequate to satisfy thermal stress requirements. Actual bolt loads will be significantly lower than those analytically predicted because of local yielding in the area of the bolt that is not included in the analysis.

### **Swivel-Stud Strength Tests**

Figure 6 summarizes four component tests that were done to demonstrate the strength of the various elements of an individual swivel-stud attachment point. The testing of the swivel-stud-to-skin bond (fig. 6(a)) was used to select and qualify an adhesive that would maintain strength at high temperatures. A 445-N load was selected as the static-load criterion. The test results for the selected adhesive indicated a 95-percent probability of holding a 445-N tensile load to a temperature greater than 271 °C using a normal statistical distribution.

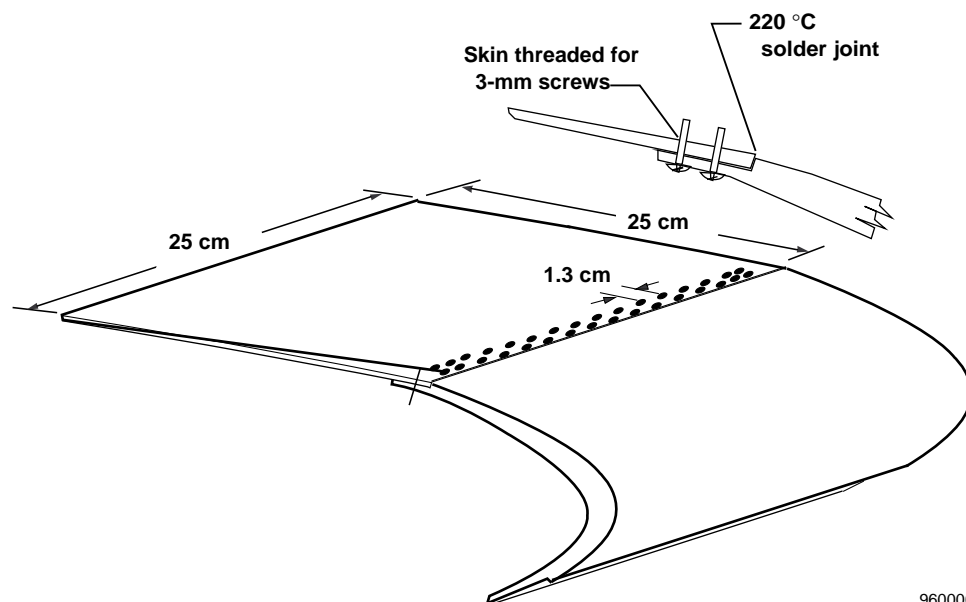


Figure 5. Upper joint test article.

960006



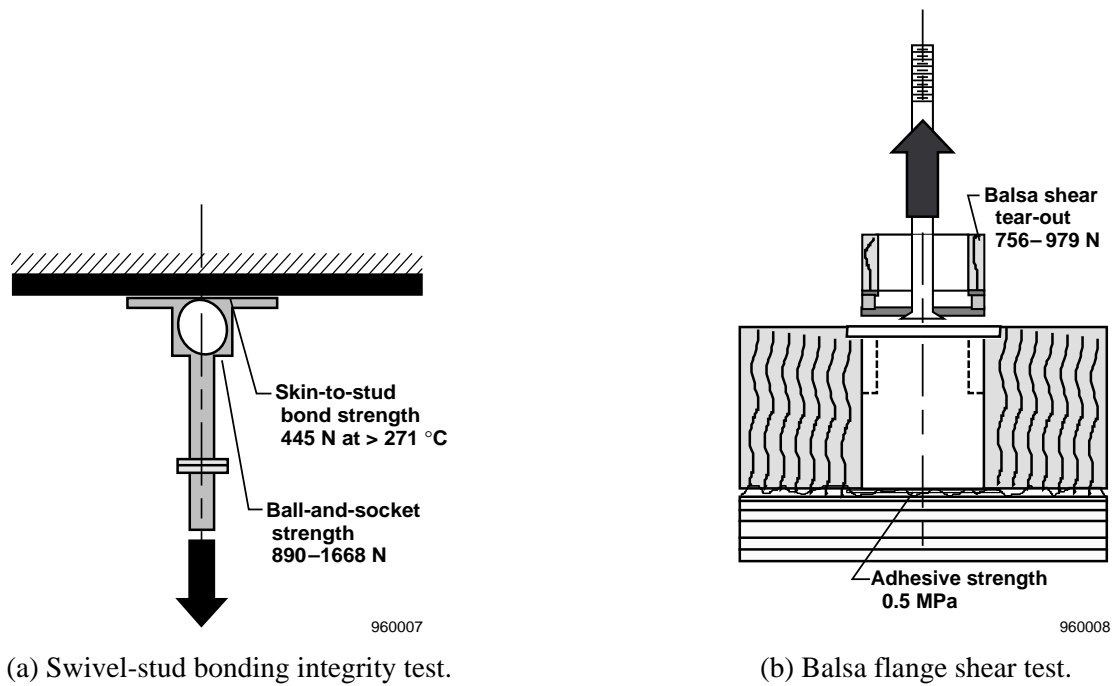


Figure 6. Small-scale laboratory tests.

The weak link in the balsa attachment was the shearing of the balsa flange that supports the swivel-stud preload springs. Figure 6(b) shows the configuration of the coupons used to test this area. The test results indicated good strength for the typical balsa flange. In some local areas, the flange depth was reduced significantly and basswood inserts were installed to increase the shear strength.

The balsa substructure of the glove is bonded to the Pegasus<sup>®</sup> wing with a polysulfide adhesive. Testing done for this joint, which includes a real wing upper-surface skin, indicated strengths well in excess of the balsa and swivel-stud strength. The demonstrated high strength ratio of the Pegasus<sup>®</sup> wing skin to foam core provides a fail-safe feature. In the unlikely event of a local overload from the glove outer skin, the studs and balsa would fail before the loads could be high enough to damage the basic wing structure.

## STRUCTURAL ANALYSES

In addition to the laboratory tests, analyses were required in the design verification process to understand those features that were nearly impossible to represent in the laboratory. The analyses were used to represent such design features as geometrically complex glove shapes, such as Bezier curves and three-dimensionally varying contours; nontrivial load conditions, such as nonuniform transient-temperature distributions; nonlinear boundary conditions, such as expansion joints and surfaces with contact and sliding friction; and nontraditional engineering materials, such as balsa wood, mechanical springs, and swivel-stud mechanisms. The analyses used a computationally intensive nonlinear solution process to determine transient stress and buckling characteristics of the glove during the experiment.

### Finite-Element Model

Figure 7 shows various views of the glove model generated with MSC/NASTRAN (version 68), Lahey, et al. (ed).<sup>6</sup> A three-dimensional finite-element model was constructed that consisted of 3777 hexahedron elements, 187 pentahedron elements, and 1194 nonlinear contact-friction elements. The model was meshed in such a way as to match the location of each swivel-stud assembly in the balsa support system. The leading-edge heat sink is modeled with solid elements to incorporate the large temperature drop through the thickness of the leading edge. The fixed restraint is located inboard (fig. 7(c)).

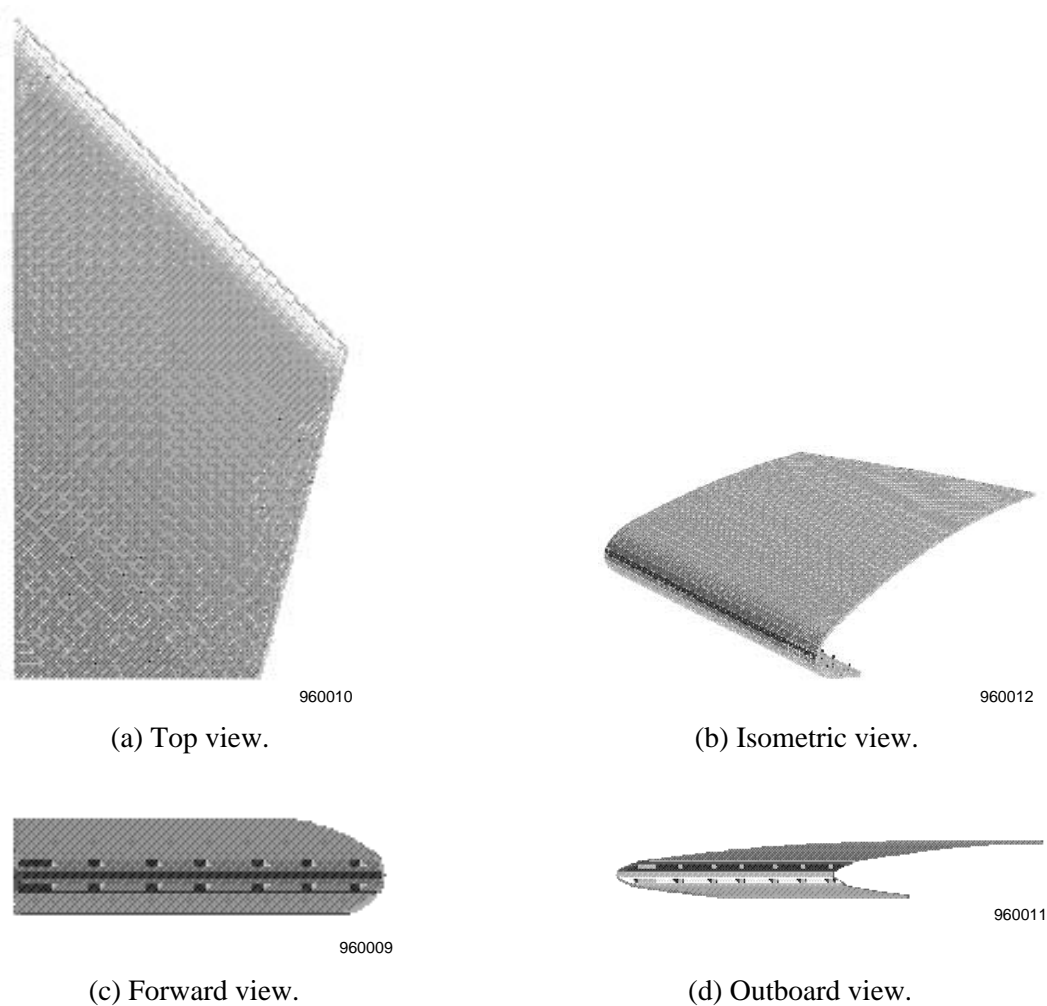


Figure 7. Finite-element model.

Linear stress analysis assumes that displacements are linearly related to the forces applied to the structure. However, this relationship does not apply at the sliding attachment boundary between the thin skin and the balsa wood support. Nonlinear, contact-friction elements, formulated to represent the balsa wood stiffness; swivel-stud assemblies; wavy springs; and the wood/skin interface were used to model this complex behavior. These elements are inherently nonlinear because at each load increment in the solution sequence, the code determines if the contact surface is stationary and resisted by static friction, if the contact surface has slipped and is resisted by kinetic friction, or if the internal element forces have exceeded the preload and the surface has opened.

### Temperature Distributions

Initially, the temperature distribution at a single time in the thermal analysis was input to a structures model to predict the stress field and buckling characteristics of the glove. The temperature distribution at 69 sec (first-stage burnout time) was initially chosen because it corresponded to the end of the heating profile when thermal stresses are usually assumed to be the most extreme. A more rigorous analysis showed that multiple times in the temperature-time history were necessary because the temperature gradients varied considerably throughout the trajectory. Therefore, analyses were also performed for times at 45, 75, and 90 sec (second-stage ignition) into the mission profile. Times of 45 and 75 sec correspond to the points at which the thermal gradient between the thick leading edge and thin skin is the most extreme.

## Boundary Conditions

The fixed boss located at the inboard area of the leading edge is the only place where the glove is rigidly attached to the wing. All degrees of freedom at this location were therefore constrained in the analysis. Displacements of the leading-edge slotted attachments were initially prevented in the direction normal to the leading edge, but were allowed in the parallel direction to accommodate the thermal expansion in this direction. However, after the stress analyses were performed at the three additional profile times, it was discovered that the original attachment scheme produced stresses greater than the acceptable yield stress criteria.

Various attachment schemes were analytically studied to help identify an acceptable attachment technique. Based on these studies, glove design modifications were made at the leading edge at the attachments and slotted joints. The displacement in the direction normal to the leading edge was allowed everywhere at the leading edge except the most inboard and most outboard leading-edge connections. Consequently, the constraints at the leading edge were similar to a simply supported beam that is able to rotate at both ends. These changes allowed greater thermal distortion at the leading edge, but were necessary to ensure the thermal stresses were less than the allowable yield stress criteria.

## RESULTS AND DISCUSSION

Stresses and displacements were predicted at multiple points in the transient heating profile. This section highlights some of the significant results from the structural analysis.

### Stress Results

Table 1 summarizes the transient stress results and factors of safety of the most critical components to the glove design. The maximum stresses induced during the trajectory are highlighted. These results were used to determine the component safety factor. As table 1 shows, the maximum stress in each of the glove components

Table 1. Stress results.

Glove component	Time, sec				Allowable stress	Factor of safety
	45	69	75	90		
	Stress results, MPa					
<u>Upper skin</u>						
Max. shear stress	82	80	84	55	241	2.9
<u>Lower skin</u>						
Max. shear stress	113	121	117	89	241	2.0
<u>Upper joint</u>						
Max. skin-shear stress	90	96	82	62	241	2.5
<u>Lower joint</u>						
Max. skin-shear stress	136	134	129	97	241	1.8
<u>Leading edge</u>						
Max. shear stress	120	104	112	118	241	2.0
Boss bearing stress	48	49	63	66	241	3.7

occurs at different times during the mission. This result underscores the need for transient analyses; conventional analyses techniques that use steady-state, linear assumptions to simplify the problem could produce erroneous predictions and nonconservative design results.

Figure 8 shows one of the component stress results shown in table 1. The shear stress in the upper joint is mapped on the glove model. The area of highest shear occurs at the inboard end of the soldered and bolted joint. The analysis did not attempt to account for additional strength provided by the solder. Despite this, all critical glove components are well below the allowable stress with a factor of safety of at least 1.5.

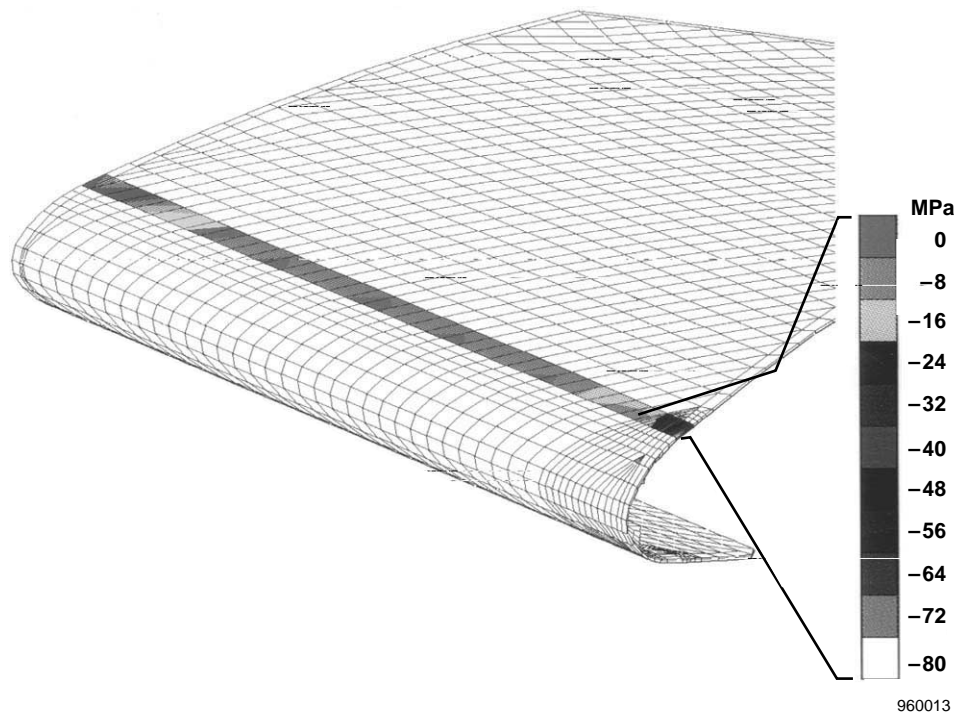
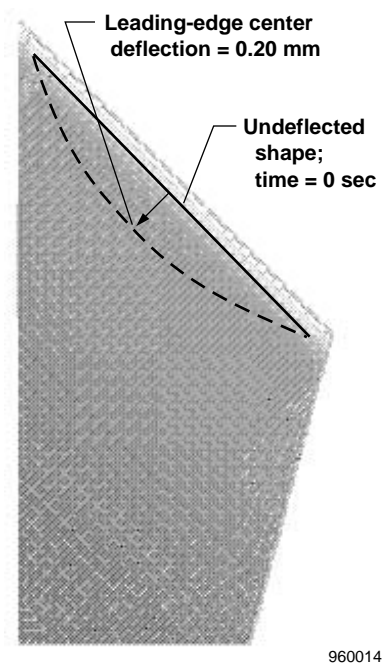


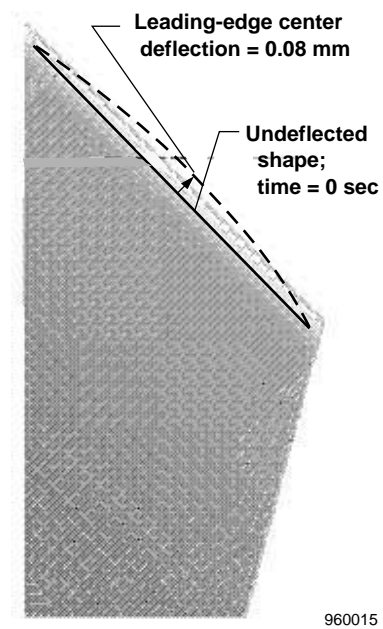
Figure 8. Shear stress in upper joint.

## Deformation Results

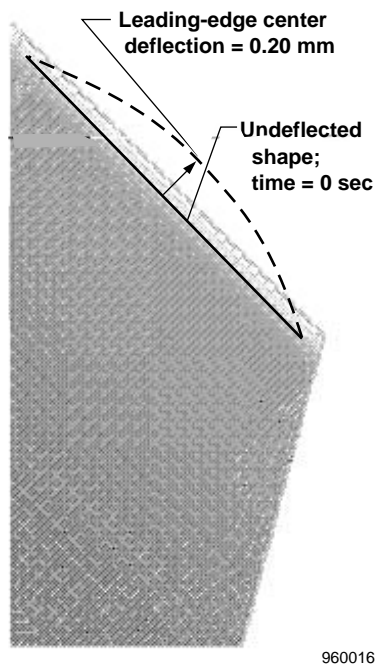
Figure 9 shows top views of the leading-edge distortion at 45, 69, 75, and 90 sec in the trajectory. This figure also illustrates why a transient structural analysis was required. The 69-sec deflection, assumed as the worst-case condition for the preliminary design, appears to be the most benign of the four times evaluated. The center leading edge thermally distorts aft at 45 sec in the profile. At 69 sec, the stagnation heating at the leading edge forces the leading-edge deflection through its initial starting point. At 75 sec, the gradient between the leading edge and thin skin has reached a displacement nearly equal in magnitude and opposite in sign to the displacement at 45 sec. At 90 sec, the displacement has bowed out to a maximum displacement of 0.03 cm. Although the maximum center deflections vary from 0.02 cm in the aft direction to 0.03 cm in the forward direction, these are well within the experiment deflection limits of 0.005 cm over a 5-cm in-plane length.



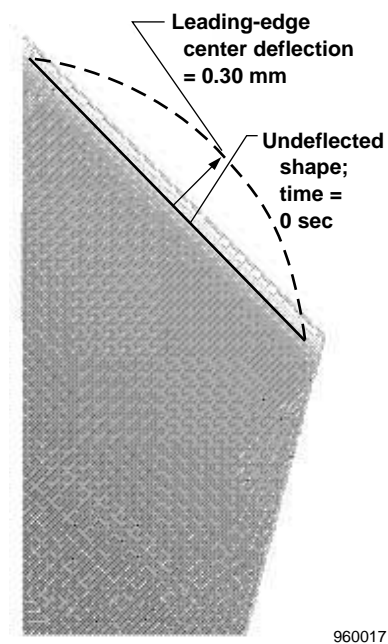
(a) Leading-edge deflection at 45 sec.



(b) Leading-edge deflection at 60 sec.



(c) Leading-edge deflection at 75 sec.



(d) Leading-edge deflection at 90 sec.

Figure 9. Leading-edge deflections at several profile times.

## CONCLUDING REMARKS

A comprehensive structural test and analysis program has been successfully completed to validate the design of a flight-test article for a Mach-8 boundary-layer experiment. The test article consisted of nontraditional engineering materials and geometrically complex components, had transient boundary conditions, and was constructed using unique manufacturing processes. Extensive small-scale laboratory testing was used to verify those areas in the glove that possessed the greatest design uncertainty or were impractical to model analytically. A three-dimensional nonlinear structural analysis was instrumental in accurately representing the complex glove characteristics during the transient flight profile reaching Mach 8. Test and analysis activities were worked in concert to help design and validate the glove test article required for the experiment. Results obtained from the structural analysis and laboratory testing were presented. These results show that all glove components are well within the allowable stress and deformation limits to satisfy experiment objectives.

## REFERENCES

1. Bertilrud, Arild, Kolodziej, Paul, Noffz, Greg K., and Godil, Afzal. *Plans for In-Flight Measurement of Hypersonic Crossflow Transition on the Pegasus<sup>®</sup> Launch Vehicle*, AIAA-92-4104, Aug. 1992.
2. Noffz, Gregory K., Curry, Robert E., Haering, Edward A., Jr., and Kolodziej, Paul. *Aerothermal Test Results From the First Flight of the Pegasus Air-Launched Space Booster*, NASA TM-4330, 1991.
3. Noffz, Gregory K., Moes, Timothy R., Haering, Edward A., Jr., and Kolodziej, Paul. *Aerothermal Test Results From the Second Flight of the Pegasus<sup>®</sup> Booster*, NASA TM-4391, 1992.
4. Gong, Leslie, Richards, W. Lance, Monaghan, Richard C., and Quinn, Robert D. *Preliminary Analysis for a Mach 8 Crossflow Transition Experiment on the Pegasus<sup>®</sup> Space Booster*, NASA TM-104272, 1993.
5. Godil, A. and Bertilrud, A. Design of a Wing Shape for Study of Hypersonic Crossflow Transition in Flight, *Computing Systems in Engineering*, Vol. 3, Nos. 1–4, pp. 115–130, Pergamon Press Ltd, Great Britain, 1992.
6. Lahey, Robert S., Miller, Mark P., and Reymond, Michael (ed), *MSC/NASTRAN Reference Manual: Version 68, Volume 1*, The MacNeal-Schwendler Corporation, USA, 1994.

REPORT DOCUMENTATION PAGE			Form Approved OMB No. 0704-0188	
Public reporting burden for this collection of information is estimated to average 1 hour per response, including the time for reviewing instructions, searching existing data sources, gathering and maintaining the data needed, and completing and reviewing the collection of information. Send comments regarding this burden estimate or any other aspect of this collection of information, including suggestions for reducing this burden, to Washington Headquarters Services, Directorate for Information Operations and Reports, 1215 Jefferson Davis Highway, Suite 1204, Arlington, VA 22202-4302, and to the Office of Management and Budget, Paperwork Reduction Project (0704-0188), Washington, DC 20503.				
1. AGENCY USE ONLY (Leave blank)		2. REPORT DATE March 1996		3. REPORT TYPE AND DATES COVERED Technical Memorandum
4. TITLE AND SUBTITLE Analytical and Experimental Verification of a Flight Article for a Mach-8 Boundary-Layer Experiment			5. FUNDING NUMBERS  WU 505-70-59	
6. AUTHOR(S)  W. Lance Richards and Richard C. Monaghan				
7. PERFORMING ORGANIZATION NAME(S) AND ADDRESS(ES)  NASA Dryden Flight Research Center P.O. Box 273 Edwards, California 93523-0273			8. PERFORMING ORGANIZATION REPORT NUMBER  H-2088	
9. SPONSORING/MONITORING AGENCY NAME(S) AND ADDRESS(ES)  National Aeronautics and Space Administration Washington, DC 20546-0001			10. SPONSORING/MONITORING AGENCY REPORT NUMBER  NASA TM-4733	
11. SUPPLEMENTARY NOTES  Presented at the First International Conference on Computational Methods and Testing for Engineering Integrity, Kuala Lumpur, Malaysia, March 19-21, 1996.				
12a. DISTRIBUTION/AVAILABILITY STATEMENT  Unclassified—Unlimited Subject Category 39			12b. DISTRIBUTION CODE	
13. ABSTRACT (Maximum 200 words)  Preparations for a boundary-layer transition experiment to be conducted on a future flight mission of the air-launched Pegasus® rocket are underway. The experiment requires a flight-test article called a glove to be attached to the wing of the Mach-8 first-stage booster. A three-dimensional, nonlinear finite-element analysis has been performed and significant small-scale laboratory testing has been accomplished to ensure the glove design integrity and quality of the experiment. Reliance on both the analysis and experiment activities has been instrumental in the success of the flight-article design. Results obtained from the structural analysis and laboratory testing show that all glove components are well within the allowable thermal stress and deformation requirements to satisfy the experiment objectives.				
14. SUBJECT TERMS  Computational methods; Flight test techniques; Structural analysis; Structural design; Structural testing			15. NUMBER OF PAGES 16	
			16. PRICE CODE AO3	
17. SECURITY CLASSIFICATION OF REPORT Unclassified	18. SECURITY CLASSIFICATION OF THIS PAGE Unclassified	19. SECURITY CLASSIFICATION OF ABSTRACT Unclassified	20. LIMITATION OF ABSTRACT  Unlimited	